Title
Coordination Polymers of 5-Alkoxy Isophthalic Acids

Journal
Crystal Growth & Design, 16(10)

ISSN
1528-7483

Authors
McCormick, Laura J
Morris, Samuel A
Slawin, Alexandra MZ
et al.

Publication Date
2016-10-05

DOI
10.1021/acs.cgd.6b00853

Peer reviewed

Coordination polymers of 5-alkoxy isophthalic acids

Laura J. McCormick,[a†]* Samuel A. Morris,[a] Alexandra M. Z. Slawin,[a] Simon J. Teat[b] and Russell E. Morris[a]

[a] School of Chemistry, University of St Andrews, North Haugh, St Andrews, Fife, Scotland, KY16 9ST, UK.

[b] Advanced Light Source, Lawrence Berkeley Laboratory, 1 Cyclotron Road, Berkeley, California 94720, USA

Abstract

The topology of coordination polymers containing 5-alkoxy isophthalic acids and first row transition metals was found to be dependent on the combination of solvent system used and length of the alkyl chain. Four different framework types were identified: Phase A $M_6(ROip)_5(OH)_2(H_2O)_4 \square x H_2O$ (M = Co and R = Et, Pr or ^{n}Bu, or M = Zn and R = Et); Phase B $M_2(ROip)_2(H_2O)$ (M = Co or Zn and R = Et, Pr, ^{n}Bu or ^{i}Bu, or M = Mn and R = ^{n}Bu or ^{i}Bu); Phase C $Zn_3(EtOip)_2(OH)_2$; and Phase D $Zn_2(EtOip)_2(H_2O)_3$. Preliminary screening of the NO storage and release capabilities of the Co-containing materials is also reported.

Introduction

The metal-organic frameworks that have received the most attention for applications-based research are all derived from the aryl carboxylic acids ligands trimesic acid (HKUST-1,[1] MIL-100-Cr[2] or –Fe[3]), or terephthalic acid (UiO-66,[4] MIL-53,[5] MIL-101,[6] MOF-5[7]) and its hydroxyl-[8-14] and amino-functionalised[15-18] derivatives. These ligands are rigid and bind predictably to the metal-based secondary building units required to generate extended coordination frameworks. Despite the structural similarities between these ligands and isophthalic acid, the related family of 5-substituted isophthalic acids have received only modest attention as potential coordination polymer/MOF precursors, particularly given the commercial availability of the 5-methyl[19-34] and 5-*tert*butyl[29,31,35-57] derivatives.

Despite the comparatively large number of coordination frameworks with reported crystal structures in which 5-methoxy isophthalic acid acts as the sole bridging ligand,[56,58-68] only two coordination frameworks have been reported to date which contain longer alkyl chain substituents on the phenolic oxygen atom.[69] The related 5-

benzyloxy isophthalic acid has received more attention, with isostructural 3D frameworks of composition $M_2(BzOip)_2(H_2O)$ (M = Co[70] or Zn[71]) prepared from aqueous solution, and a Kagome lattice of composition Cu(BzOip)(pyr).[72] We have recently undertaken investigations into synthesising novel coordination polymers derived from the 5-methyl, methoxy and *tert*butyl isophthalic acids,[61,73] and screening these materials for their ability to store and release nitric oxide (NO). Interest in the use of porous materials such as coordination frameworks[61,73-82] and zeolites[83-88] as nitric oxide delivery materials has been growing over the past decade. Nitric oxide has *in vivo* roles in wound healing and preventing the formation of thromboses, and also displays antibacterial properties.[89,90] Introduction of exogenous nitric oxide for medicinal purposes by use of gaseous nitric oxide or glyceryl trinitrate solutions does not allow for the targeted release of NO, whereas water-catalysed release of NO from porous materials allows the NO to be released where it is needed.[91]

We have conducted a systematic investigation into the coordination chemistry of the 5-ethoxy (**I**, H_2EtOip), *n*-propoxy (**II**, H_2PrOip), *n*-butoxy (**III**, $H_2{}^n$BuOip), and *i*-butoxy (**IV**, $H_2{}^i$BuOip) isophthalic acids under solvothermal conditions at 110 °C. Herein we report the synthesis and characterisation of several novel coordination frameworks containing the ligands **I** to **IV**, and preliminary NO release studies on the resulting Co-containing materials.

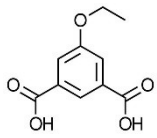

I, H_2EtOip

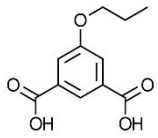

II, H_2PrOip

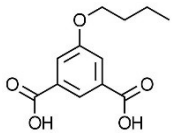

III, $H_2{}^n$BuOip

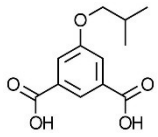

IV, $H_2{}^i$BuOip

Results and Discussion

Ligands were prepared using variations on the literature procedure.[69] The alkylation of dimethyl 5-hydroxy isophthalate was found to require longer reactions times as the length of the alkyl chain increased (R = Et required approx. 18 hours, whereas R = ^{i}Bu

required in excess of three days). NMR analysis of the products obtained for R = Pr, ^{n}Bu or ^{i}Bu showed that these solids were often a mixture of the desired dimethyl 5-alkoxy isophthalate and the starting material (up to 20% dimethyl 5-hydroxy isophthalate). Further purification proved unnecessary, as the 5-hydroxy starting material was dissolved during the subsequent saponification to the corresponding 5-alkoxy isophthalic acid, and both ^{1}H and ^{13}C NMR spectra showed that the 5-alkoxy isophthalic acids were obtained as pure products, albeit in lower yields than would be obtained from clean starting materials.

Typical coordination polymer syntheses involved solvothermal reaction of equimolar amounts of $M(OAc)_2$ (M = Mn, Co or Zn) and 5-alkoxyisophthalic acid in a solution of either water or aqueous alcohol in a 2:1 alcohol to water ratio (67% alcohol), heated to 110°C for three days. Crystallographic analysis of the resulting crystals showed that the crystals formed as one of four different frameworks: Phase A of composition $Co_6(EtOip)_5(OH)_2(H_2O)_{4.5}\cdot xH_2O$ or $M_6L_5(OH)_2(H_2O)_4\cdot xH_2O$; Phase B of composition $Co_2(EtOip)_2(H_2O)_{1.48}$ or $M_2L_2(H_2O)$; Phase C of composition $Zn_3(EtOip)_2(OH)_2$; or Phase D of composition $Zn_2(EtOip)_2(H_2O)_3$. Tables 1 and 2 show the distribution of the four phases for Co and Zn across the five different ligands and six different solvent systems. The phase impure A/B mixture produced by reaction of $Co(OAc)_2$ and $H_2{}^{n}$BuOip in aqueous methanol, and the inhomogeneous solids produced by reaction of $Co(OAc)_2$ and H_2EtOip or $H_2{}^{n}$PrOip in aqueous *n*-propanol, *iso*propanol and *tert*butanol (and $Co(OAc)_2$ and $H_2{}^{n}$BuOip in *n*-propanol) under the above conditions, are discussed in the ESI.

Solvent/Ligand	H_2EtOip	H_2PrOip	$H_2{}^{n}$BuOip	$H_2{}^{i}$BuOip
H_2O	-	-	-	B
MeOH	A	A	A/B	B
EtOH	A	A	B	B
^{i}PrOH	A/B	A/B	B	B
^{n}PrOH	A/B	A/B	B	B
^{t}BuOH	A/B	A/B	B	B

Table 1: The products prepared by reaction of various H_2ROip ligands with $Co(OAc)_2$ in different solvent mixtures. The dash symbol '-' denotes no solid product was produced that did not dissolve when washed in ethanol.

Solvent/Ligand	H_2EtOip	H_2PrOip	$H_2{}^{n}$BuOip	$H_2{}^{i}$BuOip

H_2O	B/C/D	B	B	B
MeOH	A	B	B	B
EtOH	C	B	B	B
^{i}PrOH	C	B	B	B
^{n}PrOH	C	B	B	B
^{t}BuOH	C/B	B	B	B

Table 2: The products prepared by reaction of various H_2ROip ligands with $Zn(OAc)_2$ in different solvent mixtures.

Manganese did not afford crystalline products with 5-ethoxy- or 5-propoxy isophthalic acids, Table 3 summarises the crystalline products obtained by reaction of 5-*n*- and 5-*i*-butoxy isophthalic acids only. Powder X-ray diffraction showed that the reaction between $Mn(OAc)_2$ and 5-*i*-butoxy isophthalic acid in methanol affords a crystalline product that we designate as Phase E, however this compound does not give crystals large enough for single crystal analysis. A PXRD pattern of Phase E is presented in the ESI. PXRD of the solid obtained by reaction of $H_2{}^{n}$BuOip and $Mn(OAc)_2{\cdot}4H_2O$ consistently showed the presence of a small amount of unknown contaminant.

Solvent/Ligand	$H_2{}^{n}$BuOip	$H_2{}^{i}$BuOip
H_2O	-	B
MeOH	B (contaminated)	E
EtOH	B	B
^{i}PrOH	B	B
^{n}PrOH	B	B
^{t}BuOH	B	B

Table 3: The products prepared by reaction of the two isomeric H_2BuOip ligands with $Mn(OAc)_2$ in different solvent mixtures.

Phase A

Phase A forms as a three-dimensional network of composition $Co_6(EtOip)_5(OH)_2(H_2O)_{4.5}{\square}xH_2O$ or $M_6(ROip)_5(OH)_2(H_2O)_4{\square}xH_2O$ (M = Co and R = Pr or ^{n}Bu, or M = Zn and R = Et) in monoclinic space group $P2_1/n$ with approximate unit cell dimensions $a \approx 10.94$ Å, $b \approx 28.6$ Å, $c \approx 22.8$ Å, $\square \approx 99\square$. Crystals of $Zn_6(EtOip)_5(OH)_2(H_2O)_4{\square}xH_2O$ were very thin and poorly diffracting, and did not give a satisfactory solution, however, the unit cell dimensions and PXRD pattern confirm

that this material is isostructural with the Co derivatives. The frameworks contain two distinct $M_6(OH)_2(CO_2)_{10}$ clusters, Type 1 and 2, inside which the connectivity of the M centres and bridging CO_2 units are essentially identical and the following description applies equally well to both clusters (Figure 1a and b). Each cluster contains three distinct M^{II} centres, one μ_3-OH anion and four μ_2-carboxylate groups and one μ_3-carboxylate group. The two central M^{II} centres have an octahedral coordination environment consisting of one OH anion and one μ_3-CO_2 group in the *cis* arrangement, and four μ_2-CO_2 groups. One oxygen atom from each of the two μ_3-CO_2 groups bridges these two M^{II} centres. The second, monodentate oxygen atom of these CO_2 groups bind to a tetrahedral Co centre, whose coordination environment is completed by two more CO_2 groups and an OH anion. For $Co_6(EtOip)_5(OH)_2(H_2O)_{4.5}$, a water molecule with 50% occupancy is also bound to this Co centre (Co-O 2.30(3) Å), giving it a tetrahedral/trigonal bipyramidal coordination geometry. The final distinct M^{II} centre also has an octahedral coordination environment consisting of three *mer* CO_2 groups, two *cis* terminal water molecules and the OH anion. The difference between the two clusters appears to be due only to the binding mode of one carboxylate group (Figures 1a and 1b). In the Type 1 clusters, the Co-O-C-O-Co atoms are very close to coplanar, with the angle between the two Co-O-C planes increasing with the length of the alkyl chain. The carboxylate group in the Type 2 cluster, however, is significantly twisted out of the plane (~ 80°). A comparison of the angles between the two C-O-Co planes of these carboxylate groups in Types 1 and 2 clusters are presented in Table 4.

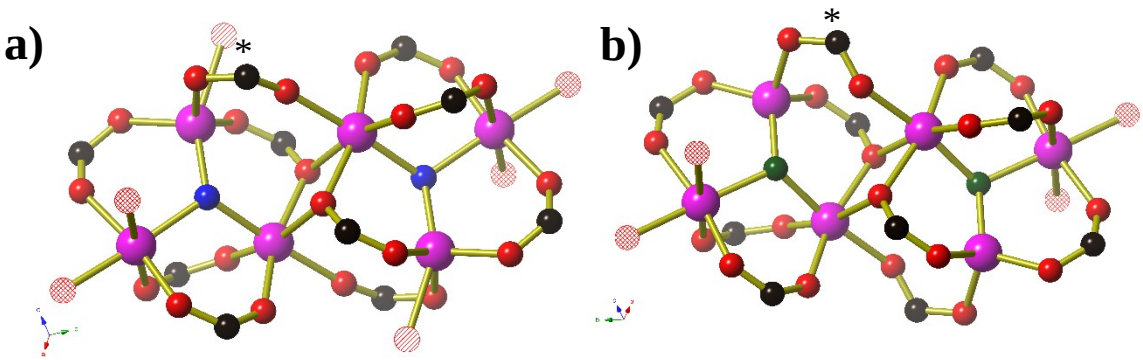

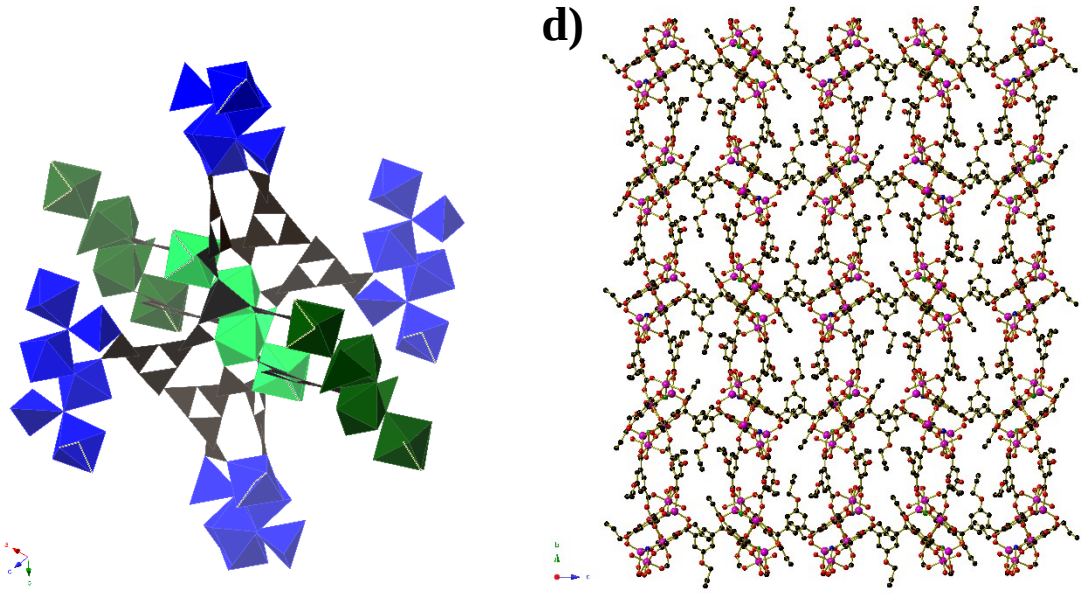

Figure 1: a) Type 1 and **b)** Type 2 clusters found in Phase A crystals $M_6(ROip)_5(OH)_2(H_2O)_n \cdot xH_2O$. The μ_3-OH anions have been coloured blue and green, respectively. Pendant water molecules are shown as hatched red spheres, whilst the partial occupancy pendant water molecules that only occur in $Co_6(EtOip)_5(OH)_2(H_2O)_{4.5}$ are shown as a striped red spheres. The carboxylate groups whose binding modes are the main difference between the two clusters are marked with an asterisk (*). **c)** The connectivity of the $M_6(OH)_2(CO_2)_{10}$ clusters. Type 1 clusters are shown using blue polyhedra and Type 2 clusters are shown using green polyhedra, the central cluster has been highlighted using a paler shade of green. The isophthalate cores of the ligands are shown as black triangles. **d)** The full network of $Co_6(PrOip)_5(OH)_2(H_2O)_4$. The μ_3-OH anions have been coloured blue and green in Type 1 and 2 clusters, respectively.

	Cluster 1	Cluster 2
Et	8.5(3)°	83(1)°
Pr	16.4(4)°	79.5(6)°
^{n}Bu	27.55(0.10)°	79.4(2)°

Table 4: Comparison of the angles between the Co-C-O planes of the carboxylate groups marked with an asterisk (*) in Figure 1 in the $Co_6(EtOip)_5(OH)_2(H_2O)_{4.5}$ and $Co_6(ROip)_5(OH)_2(H_2O)_4$ (R = Pr or ^{n}Bu).

Ten alkoxy isophthalate ligands connect each cluster to six others (Figure 1c) to form a coordination framework that has the α-polonium, or primitive cubic, topology. Each cluster binds to: two clusters of the same type and two of the opposite type, each via a pair of isophthalate ligands, that are adjacent to the central cluster along the *a*- and *b*-directions, respectively; and two clusters of the opposite type, each via a single isophthalate ligand, that neighbour the central cluster along the *c* direction. The full framework is shown in Figure 1d.

Phase B

Phase B has composition $M_2(ROip)_2(H_2O)$ or $Co_2(EtOip)_2(H_2O)_{1.48}$ crystallises in the trigonal space group $R\bar{3}$ with unit cell dimensions $a \approx 28$ Å, $c \approx 18$ Å. These compounds are isostructural with the previously reported $M_2(BzOip)_2(H_2O)$ (M = Co[70] or Zn[71]). There are two crystallographically distinct M^{II} centres in the framework - one that has square pyramidal and one that has tetrahedral coordination geometry - and two distinct isophthalate ligands. As in the Co/EtO derivative of Phase A, the Co/EtO derivative of Phase B has a slightly different coordination environment surrounding the Co centres compared to the other derivatives – the 'tetrahedral' Co centre is bound to an additional partial occupancy water molecule giving it tetrahedral/trigonal bipyramidal coordination geometry. Pairs of metal centres, one of each type, are connected by a trio of carboxylate groups into a dimer that is reminiscent of a copper acetate lantern. These have a facial arrangement about the square pyramidal M^{II} centre and one of the carboxylate oxygen atoms forms a long interaction with the square pyramidal M^{II} centre on an adjacent dimer (see Figure 2a). In $Co_2(EtOip)_2(H_2O)_{1.48}$, this interaction is short enough to be considered a coordination bond, such that the two Co centres have octahedral and tetrahedral/trigonal bipyramidal coordination geometries (Figure 2b). One of the remaining two coordination sites on the square planar M^{II} centre is occupied by a terminal water molecule. An additional μ_2-carboxylate group that binds to the remaining coordination site of a tetrahedral/trigonal pyramidal M^{II} centre on an adjacent $M_2(CO_2)_3$ unit connects the $M_2(CO_2)_3$ units into a chain that extends parallel to the *c*-axis. The isophthalate ligands radiate outwards from these chains, linking each chain to three others to give a three-dimensional honeycomb framework (Figure 2c). The walls of this framework are comprised of isophthalate ligands that are arranged into Piedfort pairs (Figure 2d). The alkoxy chains project inward from the walls towards the centre of the hexagonal channels, effectively blocking them (see Figure 2e). Most commonly, the alkyl groups are disordered over two or more orientations.

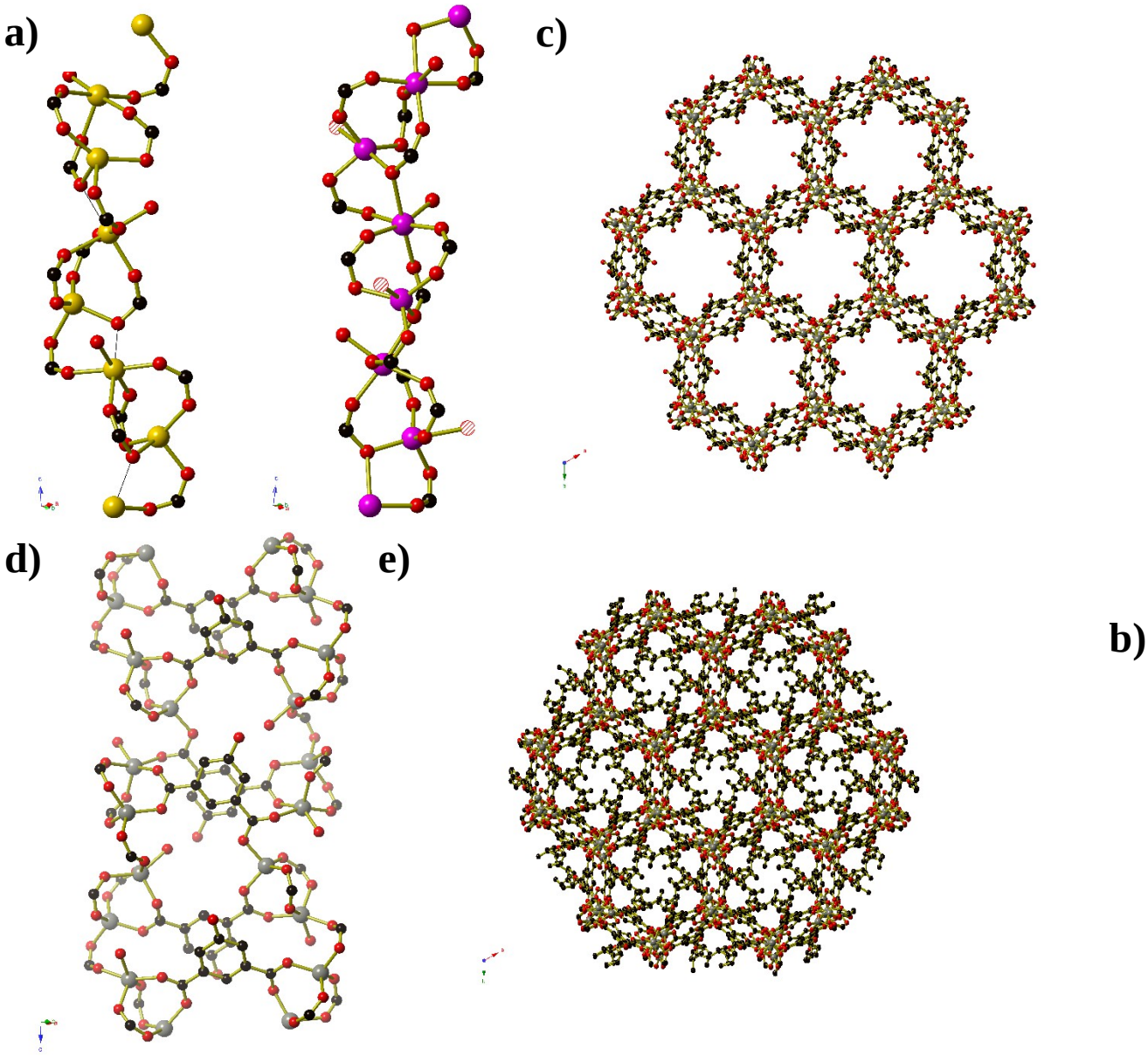

Figure 2: a) The metal-carboxylate columns found in Phase B $M_2(ROip)_2(H_2O)$. Long interactions between the metal centres and carboxylate oxygen atoms are shown as thin black lines. **b)** The metal-carboxylate columns found in Phase B $Co_2(EtOip)_2(H_2O)_{1.48}$. Partial occupancy water molecules are shown as striped red spheres. **c)** The honeycomb framework found in Phase B. The carbon atoms of the alkyl chains have been omitted for clarity. **d)** One section of the Phase B framework wall. The carbon atoms of the alkyl chains have been omitted for clarity. **e)** The full framework of $Zn_2(^{n}BuOip)_2(H_2O)$. Hydrogen atoms have been omitted for clarity.

Phase C

Phase C has composition $Zn_3(EtOip)_2(OH)_2$ and forms in triclinic space group $P\bar{1}$ with cell dimensions a = 9.182(12) Å, b = 10.973(12) Å, c = 11.761(15) Å, α = 77.69(3)°, β = 85.11(3)°, γ = 74.83(4)°. The framework is similar to that in Phase A,

in that the Zn centres are arranged into $Zn_6(OH)_2$ clusters (Figure 3a). There are three unique Zn centres within the clusters - Zn1, Zn2 and Zn3 - two hydroxide anions (Type A and B) and two $EtOip^{2-}$ ligands. Zn1 has a square pyramidal coordination environment consisting of four carboxylate oxygen atoms and one hydroxide anion, whilst both Zn2 and Zn3 have tetrahedral coordination environments consisting of two carboxylate oxygen atoms and two hydroxide anions. The $\square_3$ hydroxide anions (Type A) bridge one of each type of Zn centre into a trio, whilst carboxylate anions connect the trios into the full $Zn_6(OH)_2(CO_2)_8$ cluster. Each cluster is linked to six others to form a 3D network with the $\square$-polonium, or simple cubic, topology (Figure 3c) - pairs of $EtOip^{2-}$ ligands bridge neighbouring clusters into a sheet that extends parallel to the *bc*-plane (Figure 3b), and pairs of $\square_2$ (Type B) hydroxide anions bridge between clusters on parallel sheets (Figure 3a). PXRD analysis of the solid obtained from ^{t}BuOH shows that it is a mixture of Phases B and C (Figure 4).

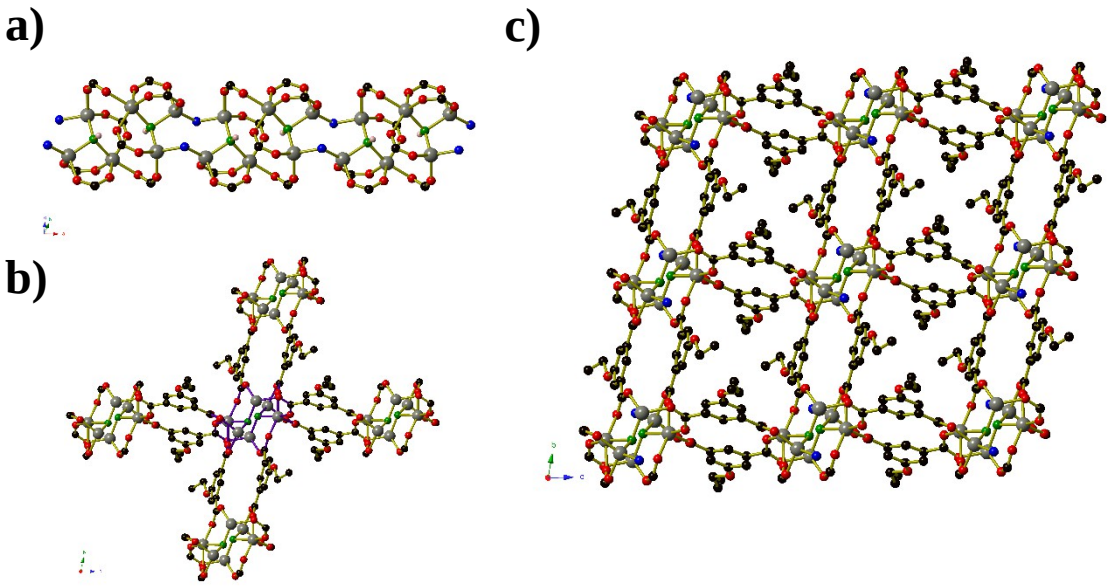

Figure 3: a) The chains of $Zn_6(OH)_2(CO_2)_8$ clusters bridged by μ_2-OH anions in Phase C . The μ_3-OH anions within the clusters are shown in green and the μ_2-OH anions that connect the clusters are shown in blue. **b)** The pairs of $EtOip^{2-}$ ligands connecting adjacent $Zn_6(OH)_2(CO_2)_8$ clusters into sheets that extend parallel to the *bc*-plane. The central $Zn_6(OH)_2(CO_2)_8$ cluster is highlighted using purple bonds. **c)** The full α-polonium framework of Phase C as viewed along the *a*-axis. Hydrogen atoms have been omitted for clarity.

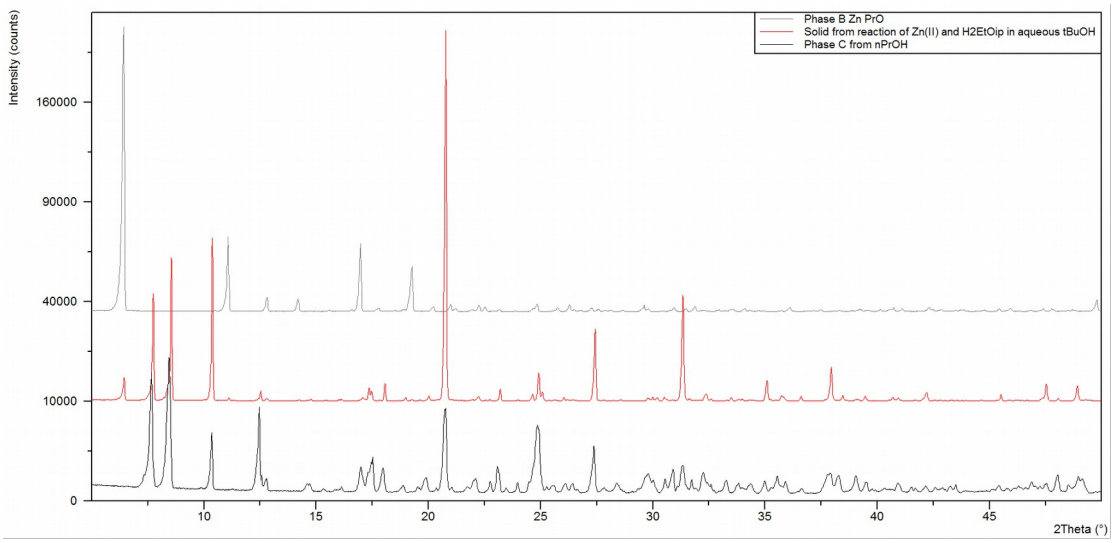

Figure 4: Comparison of the PXRD patterns of the solid obtained from reaction of $Zn(OAc)_2$ and H_2EtOip (red) from aqueous ^{t}BuOH with the experimental patterns for Phase B (grey) and Phase C (black).

Phase D

Phase D has composition $Zn_2(EtOip)_2(H_2O)_3$ and crystallises in the monoclinic space group *C*2/*c* with cell dimensions *a* = 15.101(7) Å, *b* = 15.123(7) Å, *c* = 9.652(4) Å, □ = 99.982(17)□. The compound forms as a two-dimensional framework with (4,4) topology (Figure 5b) in which the $EtOip^{2-}$ ligands act as the linear connections between four-connecting Zn_2 units. The Zn_2 units are similar to copper acetate lanterns, as may be seen in Figure 5a. All zinc centres are equivalent and have a distorted square pyramidal coordination geometry consisting of two *trans* water molecules, one monodentate carboxylate group, and two *cis* bridging carboxylate anions. All ligands are also equivalent, with one carboxylate arm connecting (along with a □$_2$ water molecule) two Zn centres into a Zn_2 lantern unit, and the second arm binding in a monodentate fashion to a second Zn_2 lantern. Unlike in similar frameworks that contain isophthalate ligands and copper acetate lantern units,[19,49,69,72,81,92-96] the arrangement of EtOip ligands about the Zn_2 lanterns produces only a single 'type' of hole passing through the sheet, one that has a hydrophilic side (with coordinated water molecules and carboxylate groups projecting into it) and a hydrophobic side (into which the ethoxy groups are directed). Sheets stack along the *c*-direction in an ABAB fashion, where the A and B layers are slightly offset from one another in the [-1 1 0] direction, such that the ethoxy isophthalate ligands in one sheet cover the hydrophilic ‘side’ of the holes in the two adjacent sheets (Figure 5c). Adjacent sheets are held together by hydrogen bonds between the terminal water

molecules on one sheet and the non-coordinated carboxylate oxygen atoms of the adjacent sheets (Figure 5d). Intra-lantern hydrogen bonds also occur between the μ_2-H_2O molecules and the non-coordinated carboxylate oxygen atoms.

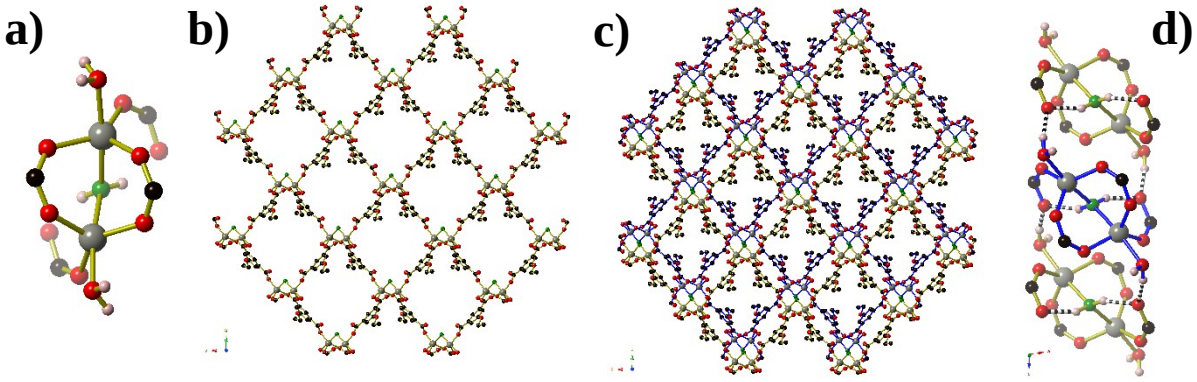

Figure 5: a) The Zn_2 lantern unit found in Phase D. The oxygen atom of the bridging water molecule is highlighted in green. **b)** One sheet of Phase D, as viewed along the *c*-axis. **c)** The ABAB stacking of sheets along the *c*-axis. The 'A' layer sheet is shown using gold bonds, the 'B' layer sheet using blue bonds. **d)** The inter-sheet hydrogen bonds between Zn_2 lanterns. Zn_2 lanterns in the 'A' and 'B' layers are shown using gold and blue bonds, respectively.

The reaction of zinc acetate with 5-ethoxy isophthalic acid in water affords a mixture of compounds B, C and D. Attempts to obtain a phase pure product by varying the reaction time from 1 to 7 days gave essentially the same mixture of products.

The preference of the system to form one phase over another in a specific solvent system we attribute to a balance of solvent and ligand polarity. The larger alkyl chains (*n*- and *i*-butyl) result in Phase B almost exclusively, in crystals of which the hydrophobic alkyl chains and hydrophilic carboxylate groups and water molecules are segregated in a manner that is reminiscent of micelle formation. This prevents the hydrophobic alkyl groups from interacting with polar solvent systems, and the hydrophilic metal-carboxylate columns from interacting with less polar solvent systems. The smallest alkyl chains (ethyl and propyl) form Phase A in polar solvent systems (methanol and, with Co^{II}, ethanol), in which the channels of the material are occupied by disordered solvent molecules and the metal sites are accessible upon dehydration (see NO release below). In solvent systems with lower polarity (propanol, *tert*butanol and, with Zn^{II}, ethanol), the segregated Phases B and C are formed. It is possible that use of even less polar alcohols, such as hexanol, may cause reaction of Co^{II} with H_2EtOip and H_2PrOip to yield pure Phase B or C, however these longer

chain alcohols are not completely miscible with water and so pose solubility issues with the metal salts.

Nitric oxide release from Phases A and B

Preliminary nitric oxide loading and release experiments were conducted on the compounds $Co_6(EtOip)_5(OH)_2(H_2O)_{4.5}$, $Co_6(PrOip)_5(OH)_2(H_2O)_4$ and $Co_6(^nBuOip)_5(OH)_2(H_2O)_4$ belonging to Phase A, and on $Co_2(^nBuOip)_2(H_2O)$ and $Co_2(^iBuOip)_2(H_2O)$ belonging to Phase B. Thermogravimetric analyses of the compounds were conducted in air and showed that decomposition for each of these samples occurred at temperatures exceeding 300ºC (see Supporting Information). Samples of a known mass ('pre-loaded weight') were dehydrated at 200°C under dynamic vacuum overnight, after which time they were exposed to 1 atm of NO for 1 hour. Excess NO was removed by vacuum, and the samples were individually flame-sealed under an argon atmosphere. Nitric oxide release was triggered by transferring NO-loaded samples into the analyser and exposing them to humid N_2 (~11% RH), and has been normalised to μmol of NO released per gram of NO-loaded sample ('loaded' weight). Further details are presented in the experimental section. The results of the NO release experiments are summarised in Tables 5 – 9, and sample NO release profiles of $Co_6(PrOip)_5(OH)_2(H_2O)_4$ and $Co_2(^iBuOip)_2(H_2O)$ are shown in Figure 6. Full NO release graphs on all runs are presented in the ESI. Co-containing samples were selected for NO release studies as Co- and Ni-CPO-27 have been shown to adsorb and deliver between 6 and 7 mmol of NO per gram of solid CPO-27 (which approximately corresponds to 1 molecule of NO per metal centre).[75]

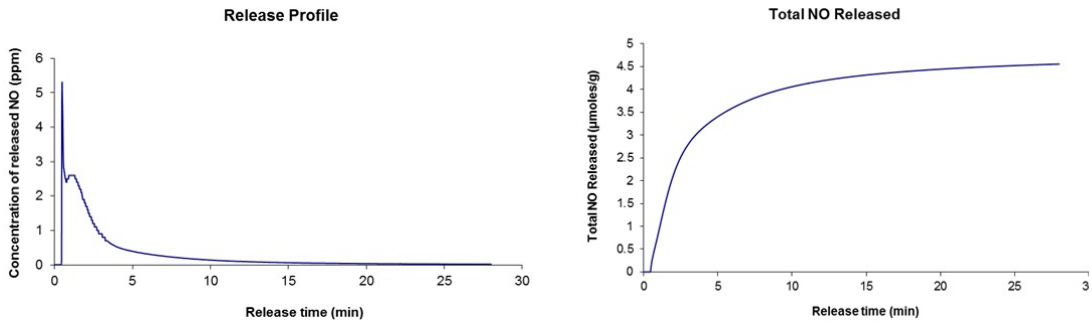

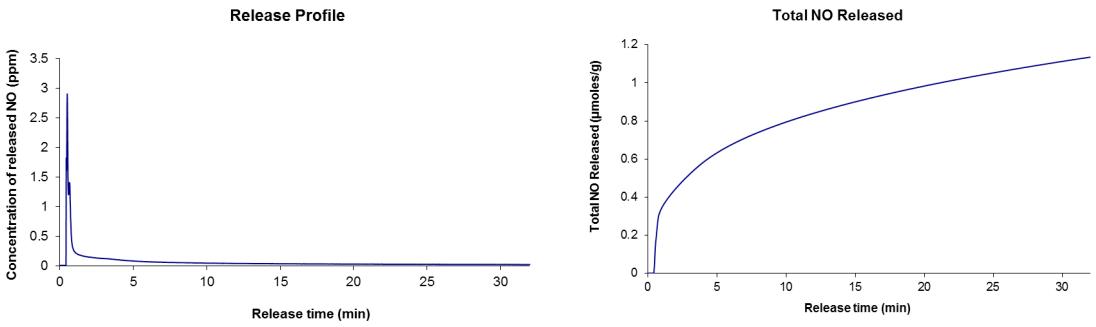

Figure 6: Graphs of NO release profile and total NO release from the sample NO release experiments on compounds $Co_6(PrOip)_5(OH)_2(H_2O)_4$ (top, Run 2) and $Co_2(^tBuOip)_2(H_2O)$ (bottom, Run 3).

The amount of NO released from Phase A is dependent on the alkyl substituent on the ligand, with the ethyl, propyl and *n*-butyl derivatives releasing an average of 1.4, 5.4 and 12.4 μmol of NO per gram of NO-loaded material, respectively, with a corresponding increase in the total release time. This was unexpected, as it was assumed that the more sterically demanding alkyl chains would block the channels and prevent the ingress and egress of the NO molecules through the materials, resulting in a smaller amount of NO released. Comparison of the PXRD patterns of the three materials before and after dehydration and NO release shows that there is no significant change in the pattern, confirming that the overall structure of the materials is either maintained throughout the NO loading and subsequent release, or that a reversible phase transition occurs. Given the dependence on the chain length displayed by the NO release of these isostructural materials, a reversible structural rearrangement was suspected and variable temperature powder X-ray diffraction studies were undertaken. The ethyl derivative was found to display a structural rearrangement upon dehydration (Figure 7), as were the propyl and *n*-butyl derivatives (see Supporting Information), that is maintained upon re-cooling the powder to room temperature. The transition is more pronounced in the ethyl derivative, most notably in the disappearance of the peaks at $2\theta \approx 3^o$ and 4.5^o (Mo Kα radiation), which would suggest that the increased steric bulk of the *n*-propyl and *n*-butyl derivatives are at least partially preventing this transition from occurring. These transitions were found to be reversible upon re-exposure to atmospheric water.

a) **b)**

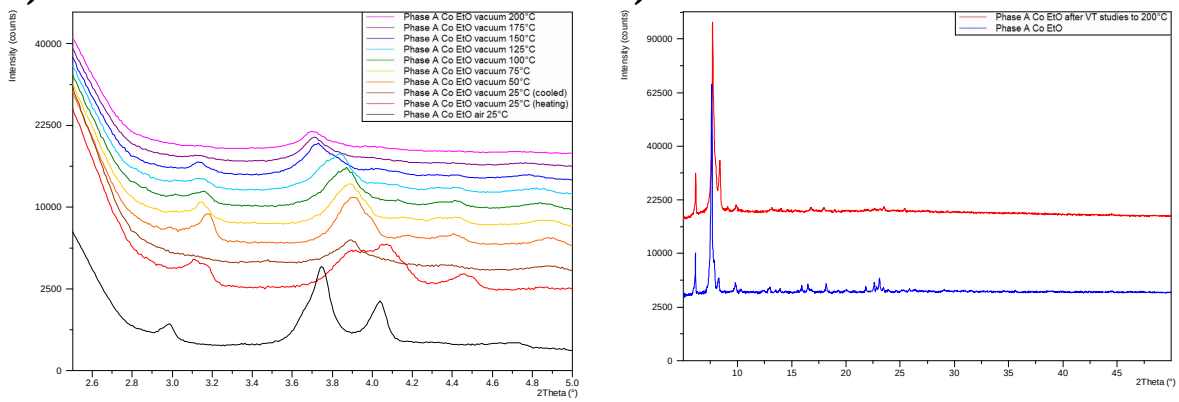

Figure 7: Variable temperature X-ray powder diffraction studies on $Co_6(EtOip)_5(OH)_2(H_2O)_{4.5}$. **a)** Individual PXRD traces on the powder at different temperatures using Mo Kα radiation shown $2.5° \leq 2\theta \leq 5.0°$. The full pattern is given in the ESI. **b)** PXRD traces on the powder before (blue) and after (red) the variable temperature PXRD studies using Cu Kα radiation.

	Pre-loaded weight (mg)	Loaded weight (mg)	Total NO release (□mol/g)	Release time (min)
1	12.6	11.0	1.15	9
2	12.8	11.4	1.33	9
3	12.9	11.4	1.45	11
4	12.7	10.7	1.42	11.5
5	12.8	10.9	1.44	10

Table 5: NO release from $Co_6(EtOip)_5(OH)_2(H_2O)_{4.5}$.

	Pre-loaded weight (mg)	Loaded weight (mg)	Total NO released (□mol/g)	Release time (min)
1	16.6	14.0	4.83	31
2	15.7	13.6	4.55	28
3	16.2	14.6	4.75	29
4	15.3	13.7	4.17	25
5	16.3	14.2	8.65	105

Table 6: NO release from $Co_6(PrOip)_5(OH)_2(H_2O)_4$.

	Pre-loaded weight (mg)	Loaded weight (mg)	Total NO release (□mol/g)	Release time (min)
1	19.8	16.9	13.01	111
2	21.0	18.6	8.75	37
3	21.2	18.7	10.73	118
4	20.8	18.4	13.03	147

5	19.9	17.8	16.41	145

Table 7: NO release from $Co_6(^{n}BuOip)_5(OH)_2(H_2O)_4$.

The amount of NO released from both butyl derivatives of Phase B is between 0.70 and 1 μmol of NO per gram of NO-loaded material. The NO release from these compounds is comparable to that observed for HKUST-1 (2 μmol/g), and even with these small amounts, NO has been shown to be biologically active in processes such as preventing platelet aggregation.[74] As with the Phase A derivatives, PXRD analysis of the Phase B materials before and after the NO-loading and release studies shows that the structure is maintained.

	Pre-loaded weight	Loaded weight	Total NO release (μmol/g)	Release time (min)
1	12.8	12.0	0.68	30
2	12.6	12.2	0.61	24
3	12.7	12.1	0.78	31

Table 8: NO release from $Co_2(^{n}BuOip)_2(H_2O)$

	Pre-loaded weight	Loaded weight	Total NO release (μmol/g)	Release time (min)
1	11.8	11.2	0.54	16
2	12.2	11.5	0.58	17
3	13.4	12.9	1.14	32
4	12.7	11.9	1.12	29
5	12.9	12.3	1.20	29

Table 9: NO release from $Co_2(^{i}BuOip)_2(H_2O)$

Conclusions

The topology of the coordination frameworks generated by reaction of a given metal acetate and 5-alkoxy isophthalic acids in aqueous alcohol was found to depend upon the combination of the alkyl chain length on both the alcohol and the alkoxy isophthalic acid. Four distinct framework topologies could be isolated (one of which could not be identified), and a further one identified as one component of a mixture of products. Initial NO release experiments suggest that the Phase A frameworks undergo a structural transition upon dehydration, which warrants further investigation.

Experimental

All reagents were obtained from commercial sources and used without further purification. The ligands were prepared using variations on the published procedures.[69] Full synthetic details of ligands and coordination frameworks are presented in ESI. Elemental analyses were conducted by the London Metropolitan University.

Crystallographic experimental details

Crystals were coated in a protective oil and mounted on a MiTeGen fibre tip (for crystals studied at the Advanced Light Source) or a Molecular dimensions mounted 0.1 mm litholoop (for crystals studied on the laboratory diffractometer). Data were collected on a Rigaku Mercury2 SCXMini diffractometer (λ = 0.71075 Å), or on a Bruker APEXII diffractometer (λ = 0.77490 Å) at station 11.3.1 of the Advanced Light Source. Appropriate scattering factors were applied using XDISP[97] within the WinGX suite.[98] Absorption corrections were applied using multi-scan methods.[99,100] Structure solutions were obtained using either SHELXS-97 or SHELXT[101] and refined by full matrix on F^2 using SHELXL-97[102] or SHELXL-2014.[103] All full occupancy non-hydrogen atoms were refined with anisotropic thermal displacement parameters. Aromatic and aliphatic hydrogen atoms were included at their geometrically estimated positions, as were hydrogen atoms bound to μ_3-OH^- anions. Hydrogen atoms belonging to free or coordinated water molecules were assigned, fixed at a distance of 0.9 Å from the oxygen atom and 1.47 Å from the second hydrogen atom of the water molecule, and their thermal parameters linked to those of the oxygen atom to which they are bound.

Ambient powder X-ray diffraction patterns were collected using Cu Kα1 radiation on PANalytical Empyrean diffractometers (Phases A, B, C, D and E) or a STOE STADIP diffractometer operating in Debye-Scherrer mode (solid from reaction of $Co(OAc)_2$ and either H_2EtOip or H_2PrOip in aqueous ^{t}BuOH). VT-PXRD studies were conducted using a PANalytical Empyrean diffractometer using MoKα1,2 radiation. VT-PXRD patterns were collected in air at 25°C, under vacuum at 25°C, and then at 25°C intervals up to 200°C, using a ramp rate of 100°C/hour with an equilibration time of 15 min prior to each measurement.

Nitric oxide sorption and release details

Individual ampules containing the powders were placed in a Schlenk flask and heated to 200°C under dynamic vacuum for approximately 18 hours. The flask was then

cooled to room temperature and exposed to an NO atmosphere (~ 1 atm static pressure) for 1 hour. Excess NO was then removed by evacuating the flask and flushing with Ar three times. The ampules were then individually flame-sealed under an argon atmosphere. NO-loaded sample masses were determined by the difference in mass of the freshly opened ampule containing the NO-loaded sample and the empty ampule after the sample has been transferred into the NO analyser. NO release measurements were performed using either a Sievers NOA 280 or 280i chemiluminescence Nitric Oxide Analyser. The instrument was calibrated using air passed through a zero filter (< 1 ppb NO) and 87.6 ppm NO gas in N_2 (Air Products). The flow rate through the instrument was set to either 200 or 180 mL/min, respectively, with a cell pressure of approximately 5.2 Torr and an O_2 pressure of 6.0 psig. Nitrogen gas of 11% R.H. was achieved by passing dry N_2 over a saturated aqueous solution of LiCl, which was then flowed over the powders at room temperature. The resulting NO/N_2 mixture was then passed into the NO analyser and the NO concentration recorded at 1 second intervals. Data collection was stopped after the concentration of NO in the carrier gas dropped below 20 ppb.

Corresponding Author

*E-mail: ljmccormick@lbl.gov; Tel: +1 510 495 2887

Present Address

†Present Address: Advanced Light Source, Lawrence Berkeley Laboratory, 1 Cyclotron Road, Berkeley, California 94720, USA

Supporting Information

Synthetic procedures; Crystal data tables for Phases A, B, C and D; Selected bonds lengths and angles for Phases A, B, C and D; Calculated and experimental PXRD spectra of all compounds; TGA traces for all phase pure materials; Further information on mixed Phase A/B solids; PXRD spectra comparison before and after NO-loading and release experiments; Graphs of NO release experiment results; Additional VT-PXRD spectra; PXRD spectra comparison on Phase A materials before and after VT-PXRD experiments

This material is available free of charge via the Internet at http://pubs.acs.org.

Acknowledgements

LJM gratefully acknowledges Dr Yuri G. Andreev for his assistance in collecting VT-PXRD spectra.

This work was funded by the British Heart Foundation (NH/11/8/29253) and the

EPSRC (EP/K005499/1). Crystallographic data for all Phase A crystals, $Co_2(EtOip)_2(H_2O)_{1.48}\square 2.06H_2O$, $Zn_2(EtOip)_2(H_2O)$, and $Mn_2(^nBuOip)_2(H_2O)$ were collected at station 11.3.1 at the Advanced Light Source, Berkeley, CA, USA. The Advanced Light Source is supported by the Director, Office of Science, Office of Basic Energy Sciences, of the U.S. Department of Energy under Contract No. DE-AC02-05CH11231.

CCDC 1479999 - 1480013 contain the supplementary crystallographic data for this paper. These data can be obtained free of charge from The Cambridge Crystallographic Data Centre via www.ccdc.cam.ac.uk/data_request/cif

References

1. S. S.-Y. Chui, S. M.-F. Lo, J. P. H. Charmant, A. G. Orpen and I. D. Williams; *Science*, 1999, **283**, 1148-1150
2. G. Ferey, C. Serre, C. Mellot-Draznieks, F. Millange, S. Surble, J. Dutour and I.Margiolaki, *Angew. Chem., Int. Ed.*, 2004, **43**, 6296-6301
3. P. Horcajada, S. Surble, C. Serre, D.-Y. Hong, Y.-K. Seo, J.-S. Chang, J.-M. Greneche, I. Margiolaki and G. Ferey, *Chem. Commun.*, 2007, 2820-2822
4. J. H. Cavka, S. Jakobsen, U. Olsbye, N. Guillou, C. Lamberti, S. Bordiga and K. P. Lillerud; *J. Am. Chem. Soc.*, 2008, **130**, 13850-13851
5. C. Serre, F. Millange, C. Thouvenot, M. Nogues, G. Marsolier, D. Louer and G.Ferey, *J. Am. Chem. Soc.*, 2002, **124**, 13519-13526
6. G. Ferey, C. Mellot-Draznieks, C. Serre, F. Millange, J. Dutour, S. Surble and I. Margiolaki, *Science*, 2005, **309**, 2040-2042
7. H. Li, M. Eddaoudi, M. O'Keeffe and O. M. Yaghi, *Nature*, 1999, **402**, 276-279
8. P. D. C. Dietzel, R. Blom and H.Fjellvåg, *Eur. J. Inorg. Chem.*, 2008, 3624-3632
9. Q. Gao, F.-L. Jiang, M.-Y. Wu, Y.-G. Huang, W. Wei, Q.-F. Zhang and M.-C. Hong, *Aust. J. Chem.*, 2010, **63**, 286-292
10. E. D. Bloch, L. J. Murray, W. L. Queen, S. Chavan, S. N. Maximoff, J. P. Bigi, R. Krishna, V. K. Peterson, F. Grandjean, G. J. Long, B. Smit, S. Bordiga, C. M Brown and J. R. Long, *J. Am. Chem. Soc.*, 2011, **133**, 14814-14822
11. P. D. C. Dietzel, Y. Morita, R. Blom and H. Fjellvåg,. *Angew. Chem., Int. Ed.*, 2005, **44**, 6354-6358
12. P. D. C. Dietzel, B. Panella, M. Hirscher, R. Blom and H. Fjellvåg, *Chem. Commun.*, 2006, 959-961
13. R. Sanz, F. Martínez, G. Orcajo, L. Wojtasc and D. Brionesa, *Dalton Trans.*, 2013, **42**, 2392-2398

14. N. L. Rosi, J. Kim, M. Eddaoudi, B. Chen, M. O'Keeffe and O. M. Yaghi; *J. Am. Chem. Soc.*, 2005, **127**, 1504-1518
15. M. Eddaoudi, J. Kim, N. Rosi, D. Vodak, J. Wachter, M. O'Keeffe and O. M. Yaghi, *Science*, 2002, **295**, 469-472
16. C. G. Silva, I. Luz, F. X. Llabres I Xamena, A. Corma and H. Gercia, *Chem. Eur. J.*, 2010, **16**, 11133-11138
17. T. Ahnfeldt, D. Gunzelmann, T. Loiseau, D. Hirsemann, J. Senker, G. Ferey and N. Stock, *Inorg. Chem.*, 2009, **48**, 3057-3064
18. S. Biswas, S. Couck, M. Grzywa, J. F. M. Denayer, D. Volkmer and P. van der Poot, *Eur. J. Inorg. Chem.*, 2012, **2012**, 2481-2486
19. R.-Q. Zou, H. Sakurai, S. Han, R.-Q. Zhong and Q. Xu, *J. Am. Chem. Soc.*, 2007, **129**, 8402-8403
20. Z.-L. Yu and J.-L. Hu, *Acta Crystallogr., Sect. E: Struct. Rep. Online*, 2008, **64**, m1522
21. H. Chun and H. Jung, *Inorg. Chem.*, 2009, **48**, 417-419
22. W.-X. Chen, Y.-P. Ren, L.-S. Long, R.-B. Huang and L.-S. Zheng, *CrystEngComm*, 2009, **11**, 1522-1525
23. L. Wang, J. Liu, C.-Z. Zheng and Y.-J. Wang, *Huaxue Yu Shengwu Gongcheng (Chem. Bioeng.)*, 2011, 17-20
24. Q.-B. Bo, Z.-W. Zhang, J.-L. Miao, D.-Q. Wang and G.-X. Sun, *CrystEngComm*, 2011, **13**, 1765-1767
25. Q.-B. Bo, H.-Y. Wang, D.-Q. Wang, Z.-W. Zhang, J.-L. Miao and G.-X. Sun, *Inorg. Chem.*, 2011, **50**, 10163-10177
26. H. Y. Zhu, J. W. Ji, Y. W. Li, C. W. Li and K. Z. Zhu, *Koord. Khim.*, 2012, **38**, 149-152
27. J.-W. Ji, X.-F. Wang, B.-Y. Li and Z.-B. Han, *Solid State Sci.*, 2012, **14**, 335-340
28. S. Du, C. Hu, J.-C. Xiao, H. Tan and W. Liao, *Chem. Commun.*, 2012, **48**, 9177-9179
29. Q.-B. Bo, H.-Y. Wang, J.-L. Miao and D.-Q. Wang, *RSC Adv.*, 2012, **2**, 11650-11652
30. X.-L. Deng, S.-Y. Yang, R.-F. Jin, J. Tao, C.-Q. Wu, Z.-L. Li, L.-S. Long, R.-B. Huang and L.-S. Zheng, *Polyhedron*, 2013, **50**, 219-228
31. Q.-B. Bo, H.-Y. Wang and D.-Q. Wang, *New J. Chem.*, 2013, **37**, 380-390
32. L.-P. Xue, Y.-C. Liu, Y.-H. Han, C.-B. Tin, Q.-P. Li, P. Lin and S.-W. Du, *Chin. J. Struct. Chem.*, 2014, **33**, 1191-1198
33. C.-B. Tian, R.-P. Chen, C. He, W.-J. Li, Q. Wei, X.-D. Zhang and S.-W. Du, *Chem. Commun.*, 2014, **50**, 1915-1917
34. L. Jin, L.-L. Zha, S. Gao, S.-Y. Yang and R.-B. Huang, *Acta Crystallogr., Sect. E: Struct. Rep. Online*, 2015, **71**, m1-m2

35. L. Pan, B. Parker, X. Huang, D. H. Olson, J. Y. Lee and J. Li, *J. Am. Chem. Soc.*, 2006, **128**, 4180-4181
36. S. Ma, D. Sun, X.-S. Wang and H.-C. Zhou, *Angew. Chem., Int. Ed.*, 2007, **46**, 2458-2462
37. X.-L. Li and M.-L. Huang, *Acta Crystallogr., Sect. E: Struct. Rep. Online*, 2008, **64**, m1501-m1502
38. X.-L. Li and M.-L. Huang, *Z. Kristallogr. - New Cryst. Struct.*, 2009, **224**, 127-128
39. Y.-T. Fan, B. Li, L.-F. Ma and L.-Y. Wang, *Chin. J. Struct. Chem.*, 2009, **28**, 1061-1066
40. Z.-X. Du, L.-Y. Wang and H.-W. Hou, Z. *Anorg. Allg. Chem.*, 2009, **635**, 1659-1663
41. L.-F. Ma, L.-Y. Wang, D.-H. Lu, S. R. Batten and J.-G. Wang, *Cryst. Growth Des.*, 2009, **9**, 1741-1749
42. D.-S. Zhou, F.-K. Wang, S.-Y. Yang, Z.-X. Xie and R.-B. Huang, *CrystEngComm*, 2009, **11**, 2548-2554
43. J.-D. Lin, X.-F. Long, P. Lin and S.-W. Du, *Cryst. Growth Des.*, 2010, **10**, 146-157
44. J.-R. Li and H.-C. Zhou, *Nat. Chem.*, 2010, **2**, 893-898
45. J.-D. Lin, S.-T. Wu, Z.-H. Li and S.-W. Du, *Dalton Trans.*, 2010, **39**, 10719-10728
46. C.-B. Tian, Z.-Z. He, Z.-H. Li, P. Lin and S.-W. Du, *CrystEngComm*, 2011, **13**, 3080-3086
47. B. Kilbas, S. Mirtschin, T. Riis-Johannessen, R. Scopelliti and K. Severin, *Inorg. Chem.*, 2012, **51**, 5795-5804
48. L.-J. Chen, J.-B. Su, R.-B. Huang, S. Lin, M.-X. Yang and H. Huang, *Dalton Trans.*, 2011, **40**, 9731-9736
49. X.-F. Wang, L. Li, Y.-M. Kong and Y. Liu, *Inorg. Chem. Commun.*, 2012, **21**, 72-75
50. S.-H. Li and J.-B. Guo, *Z. Kristallogr. - New Cryst. Struct.*, 2012, **227**, 389-391
51. Y.-F. Liang, Y.-R. Zhang and Z.-B. Han, *Z. Anorg. Allg. Chem.*, 2012, **638**, 423-426
52. R.-F. Jin, S.-Y. Yang, H.-M. Li, L.-S. Long, R.-B. Huang and L.-S. Zheng, *CrystEngComm*, 2012, **14**, 1301-1316
53. S.-Y. Yang, H.-B. Yuan, X.-B. Xu and R.-B. Huang, *Inorg. Chim. Acta*, 2013, **403**, 53-62
54. K. Noh and J. Kim, *Acta Crystallogr., Sect. E: Struct. Rep. Online*, 2013, **69**, m579-m580

55. J. Wang, J.-Q. Tao, X.-J. Xu and C.-Y. Tan, *J. Struct. Chem.*, 2013, **54**, 805-809
56. C. Tian, Z. Lin and S. Du, *Cryst. Growth Des.*, 2013, **13**, 3746-3753
57. A. K. Chaudhari, S. Mukherjee, S. S. Nagarkar, B. Joarder and S. K. Ghosh, *CrystEngComm*, 2013, **15**, 9465-9471
58. D. Braga, S. D'Agostino and F.Grepioni, *CrystEngComm*, 2011, **13**, 1366-1372
59. H. Reinsch, M. A. van der Veen, B. Gil, B. Marszalek, T. Verbiest, D. de Vos and N.Stock, *Chem. Mater.*, 2013, **25**, 17-26
60. X.-D. Li and X.-Y. Yang, *Z. Kristallogr. – New Cryst. Struct.*, 2010, **225**, 493-494
61. L. J. M^{c}Cormick, S. A. Morris, S. J. Teat, M. J. McPherson, A. M. Z. Slawin and R. E. Morris, *Dalton Trans.*, 2015, **44**, 17686-17695
62. F.-P. Liang, Q.-L. Meng, L.-F. Ma and L.-Y. Wang, *Jiegou Huaxue (Chin. J. Struct. Chem.)*, 2010, **29**, 157-163
63. X.-H. Chang, J.-H. Qin, M.-L. Han, L.-F. Ma and L.-Y. Wang, *CrystEngComm*, 2014, **16**, 870-882
64. H.-J. Zhang, *Z. Kristallogr. - New Cryst. Struct.*, 2011, **226**, 629-630
65. X.-H. Huang, *Acta Crystallogr., Sect. C: Cryst. Struct. Commun.*, 2013, **69**, 483-485
66. A. Dorazco-Gonzalez, S. Martinez-Vargas, S. Hernandez-Ortega and J. Valdes-Martinez, *CrystEngComm*, 2013, **15**, 5961-5968
67. D. Feng, K. Wang, Z. Wei, Y.-P. Chen, C. M. Simon, R. Arvapally, R. L. Martin, M. Bosch, T.-F. Liu, S. Fordham, D. Yuan, M. A. Omary, M. Haranczyk, B. Smit and H.-C. Zhou; *Nature Comm.*, 2014, **5**, 5723
68. S.-M. Shen; *Acta Crystallogr., Sect. E: Struct. Rep. Online*, 2009, **65**, m1173
69. H. Abourahma, G. J. Bodwell, J. Lu, B. Moulton, I. R. Pottie, R. B. Walsh and M.J.Zaworotko, *Cryst. Growth Des.*, 2003, **3**, 513-519
70. X. Li, J. Li, M.-K. Li and Z. Fei, *J. Mol. Struct.*, 2014, **1059**, 294-298
71. X. Zhang, J.-X. Yang and Y.-G. Yao, *J. Inorg. Organomet. Polym. Mater.*, 2012, **22**, 1189-1193
72. J. J. Perry, G. J. M^{c}Manus and M. J. Zaworotko, *Chem. Commun.*, 2004, 2534-2535
73. L. J. M^{c}Cormick, S. A. Morris, A. M. Z. Slawin, S. J. Teat and R. E. Morris, *CrystEngComm*, 2016, **18**, 1123-1132
74. B. Xiao, P. S. Wheatley, X. Zhao, A. J. Fletcher, S. Fox, A. G. Rossi, I. L. Megson, S. Bordiga, L. Regli, K. M. Thomas and R. E. Morris, *J. Am. Chem. Soc.*, 2007, **129**, 1203-1209
75. A. C. McKinlay, B. Xiao, D. S. Wragg, P. S. Wheatley, I. L. Megson and R. E. Morris, *J. Am. Chem. Soc.*, 2008, **130**, 10440-10444

76. J. G. Nguyen, K. K. Tanabe and S. M. Cohen, *CrystEngComm*, 2010, **12**, 2335-2338
77. A. C. McKinlay, J. F. Eubank, S. Wuttke, B. Xiao, P. S. Wheatley, P. Bazin, J.-C. Lavalley, M. Daturi, A. Vimont, G. de Weireld, P. Horcajada, C. Serre and R. E. Morris, *Chem. Mater.*, 2013, **25**, 1592-1599
78. F. R. S. Lucena, L. C. C. de Araujo, M. do D. Rodrigues, T. G. da Silva, V. R. A. Pereira, G. C. G. Militao, D. A. F. Fontes, P. J. Rolim-Neto, F. F. da Silva and S. C. Nascimento, *Biomed and Pharmacotherapy*, 2013, **67**, 707-713
79. S. R. Miller, E. Alvarez, L. Fradcourt, T. Devic, S. Wuttke, P. S. Wheatley, N. Steunou, C. Bonhomme, C. Gervais, D. Laurencin, R. E. Morris, A. Vimont, M. Daturi, P. Horcajada and C. Serre, *Chem. Commun.*, 2013, **49**, 7773-7775
80. J. L. Harding and M. M. Reynolds, *J. Mater Chem. B: Mater Biol. Med.*, 2014, **2**, 2530-2536
81. M. I. H. Mohideen, B. Xiao, P. S. Wheatley, A. C. McKinlay, Y. Li, A. M. Z. Slawin, D. W. Aldous, N. F. Cessford, T. Düren, X. Zhao, R. Gill, K. M. Thomas, J. M. Griffin, S. E. Ashbrook and R. E. Morris, *Nature Chem.*, 2011, **3**, 304-310
82. K. Peikert, L. J. M^{c}Cormick, D. Cattaneo, M. J. Duncan, F. Hoffmann, A. H. Khan, M. Bertmer, R. E. Morris and M. Fröba, *Microporous and Mesoporous Materials*, 2015, **216**, 118-126
83. P. S. Wheatley, A. R. Butler, M. S. Crane, S. Fox, B. Xiao, A. G. Rosse, I. L. Megson and R. E. Morris, *J. Am. Chem. Soc.*, 2006, **128**, 502-509
84. B. Xiao, P. S. Wheatley and R. E. Morris, *Studies Surf Sci. Cat.*, 2007, **170A**, 902-909
85. M. Mowbray, X. J. Tan, P. S. Wheatley, A. G. Rossi, R. E. Morris and R. B. Weller, *J. Invest. Derm.*, 2008, **128**, 352-360
86. H. A. Liu and K. J. Balkus, *Chem. Mater.*, 2009, **21**, 5032-5041
87. G. Narin, C. B. Albayrak and S. Ulku, *Appl. Clay Sci.*, 2010, **50**, 560-568
88. M. L. Pinto, A. C. Fernandes, J. Rocha, A. Ferreira, F. Antunes and J. Pires, *J. Mater. Chem. B: Mater. Biol. Med.*, 2014, **2**, 224-230
89. H. F. Zhu, B. Ka and F. Murad, *World J. Surg.*, 2007, **31**, 624-631
90. M. R. Miller and I. L. Megson, *Brit. J. Pharmacol.*, 2007, **151**, 305-321
91. R. E. Morris and P. S. Wheatley, *Angew. Chem,. Int. Ed.*, 2008, **47**, 4966-4981
92. L. Gao, B. Zhao, G. Li, Z. Shi and S. Feng, *Inorg. Chem. Commun.*, 2003, **6**, 1249-1251
93. M. Tonigold and D. Volkmer, *Inorg. Chim. Acta*, 2010, **363**, 4220-4229
94. H. Sato, W. Kosaka, R. Matsuda, A. Hori, Y. Hijikata, R. V. Belosludov, S. Sakaki, M. Takata and S. Kitagawa, *Science*, 2014, **343**, 167-170
95. A. Mallick, B. Garai, D. Diaz Diaz, R. Banerjee, *Angew. Chem., Int. Ed.*, 2013, **52**, 13755-13759

96. X. Li and Q. Liu, *Z. Anorg. Allg. Chem.*, 2013, **639**, 1815-1820
97. XDISP Program in WinGX, L. Kissel and R. H. Pratt, *Acta Cryst*, 1990, **A46**, 170
98. L. J. Farrugia, *J. Appl. Cryst.*, 2012, **45**, 849-854
99. SADABS: Area-Detector Absorption Correction; Siemens Industrial Automation, Inc.: Madison, WI, 1996
100. CrystalClear 2.1, Rigaku Corporation, CrystalClear Software User's Guide, Molecular Structure Corporation, 2014
101. G. M. Sheldrick, *Acta Cryst.*, 2015, **A71**, 3-8
102. G. M. Sheldrick, *Acta Crystallogr., Sect. A*, 2008, **64**, 112
103. G. M. Sheldrick, *Acta Cryst.*, 2015, **C71**, 3-8

FOR TABLE OF CONTENTS USE ONLY

Coordination polymers of 5-alkoxy isophthalic acids

Laura J. McCormick,[a†]* Samuel A. Morris,[a] Alexandra M. Z. Slawin,[a] Simon J. Teat[b] and Russell E. Morris[a]

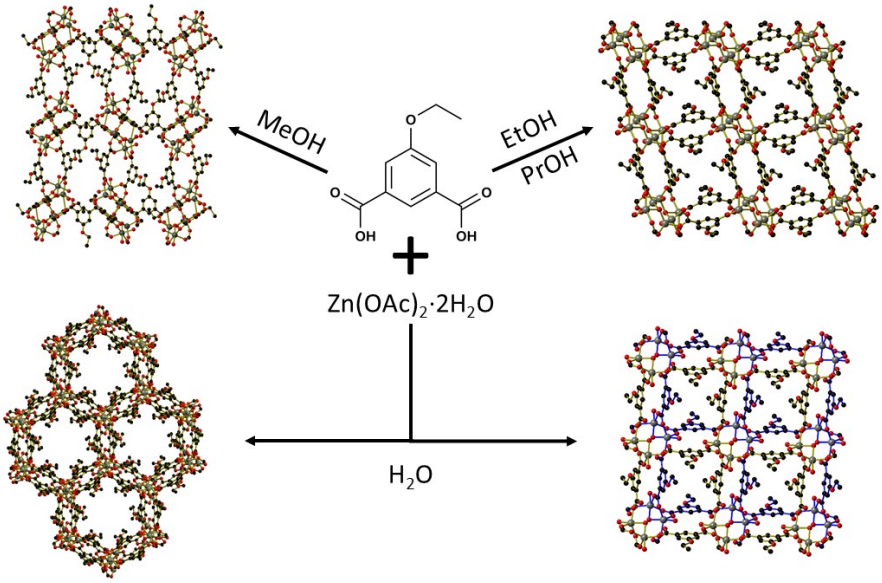

The topology of coordination polymers containing 5-alkoxy isophthalic acids and first row transition metals was found to be dependent on the combination of solvent system used and length of the alkyl chain. Four different framework types were identified: Phase A $M_6(ROip)_5(OH)_2(H_2O)_4 \square xH_2O$ (M = Co and R = Et, Pr or ^{n}Bu, or M = Zn and R = Et); Phase B $M_2(ROip)_2(H_2O)$ (M = Co or Zn and R = Et, Pr, ^{n}Bu or ^{i}Bu, or M = Mn and R = ^{n}Bu or ^{i}Bu); Phase C $Zn_3(EtOip)_2(OH)_2$; and Phase D $Zn_2(EtOip)_2(H_2O)_3$. Preliminary screening of the NO storage and release capabilities of the Co-containing materials is also reported.